Science Advances
AAAS

advances.sciencemag.org/cgi/content/full/6/19/eaay4313/DC1

Supplementary Materials for

Axonal Na^+ channels detect and transmit levels of input synchrony in local brain circuits

Mickaël Zbili*, Sylvain Rama*, Pierre Yger, Yanis Inglebert, Norah Boumedine-Guignon, Laure Fronzaroli-Moliniere, Romain Brette, Michaël Russier, Dominique Debanne*

*Corresponding author. Email: dominique.debanne@inserm.fr (D.D.); zbili.mickael@gmail.com (M.Z.); rama.sylvain@gmail.com (S.R.)

Published 6 May 2020, *Sci. Adv.* **6**, eaay4313 (2020)
DOI: 10.1126/sciadv.aay4313

This PDF file includes:

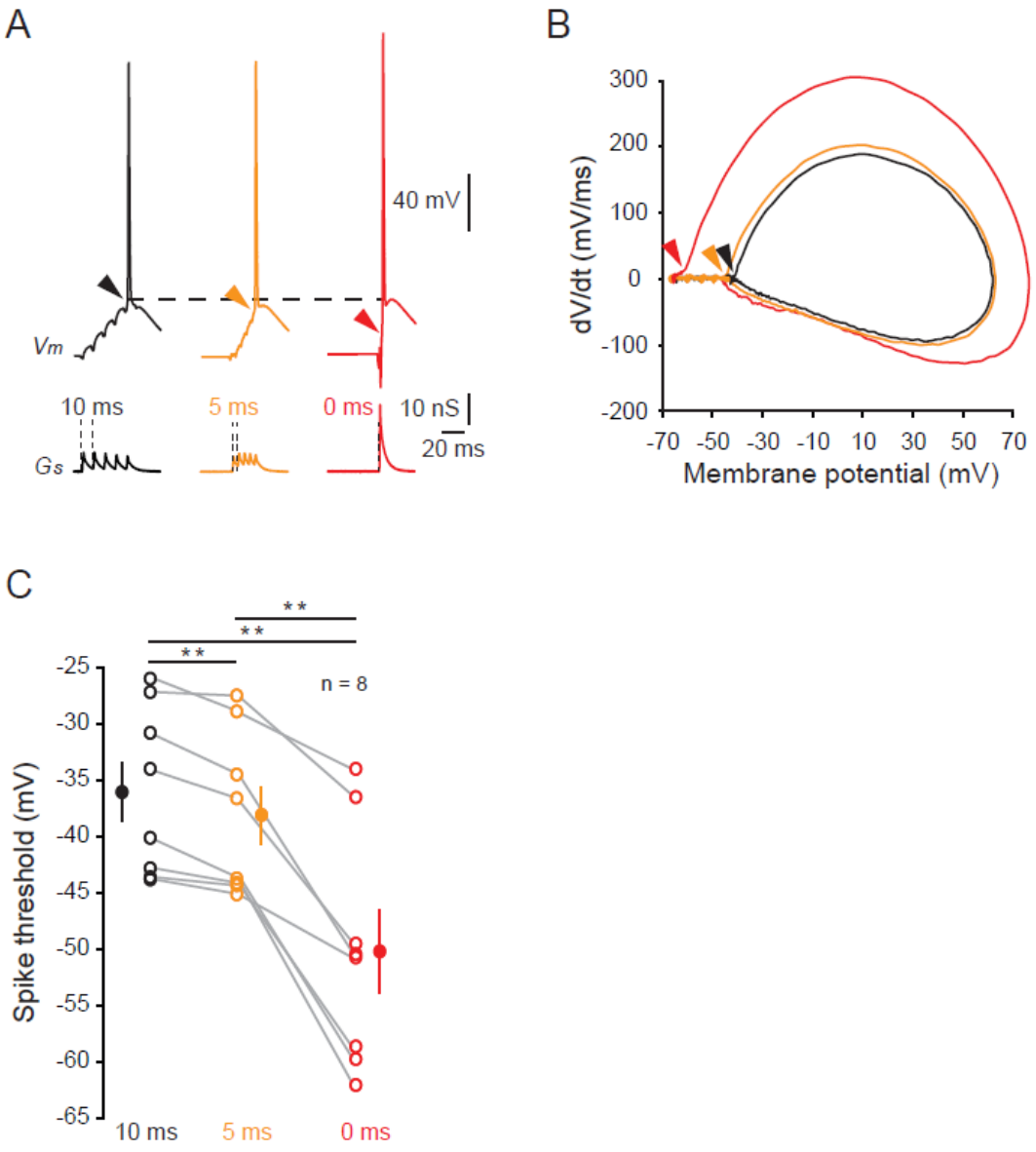

Fig. S1. Input synchrony lowers presynaptic AP threshold.
A. Experimental paradigm and action potentials triggered by various degree of input synchrony (black: 10 ms, orange: 5 ms and red: 0 ms). Resting membrane potential of the presynaptic neuron: -78 mV. **B.** Phase plots of the APs in the 3 conditions, note the hyperpolarization of the AP threshold (arrowhead) for the maximal input synchrony (red). **C.** Data analysis. **, Wilcoxon test, $p<0.01$. Friedman test, $p<0.01$.

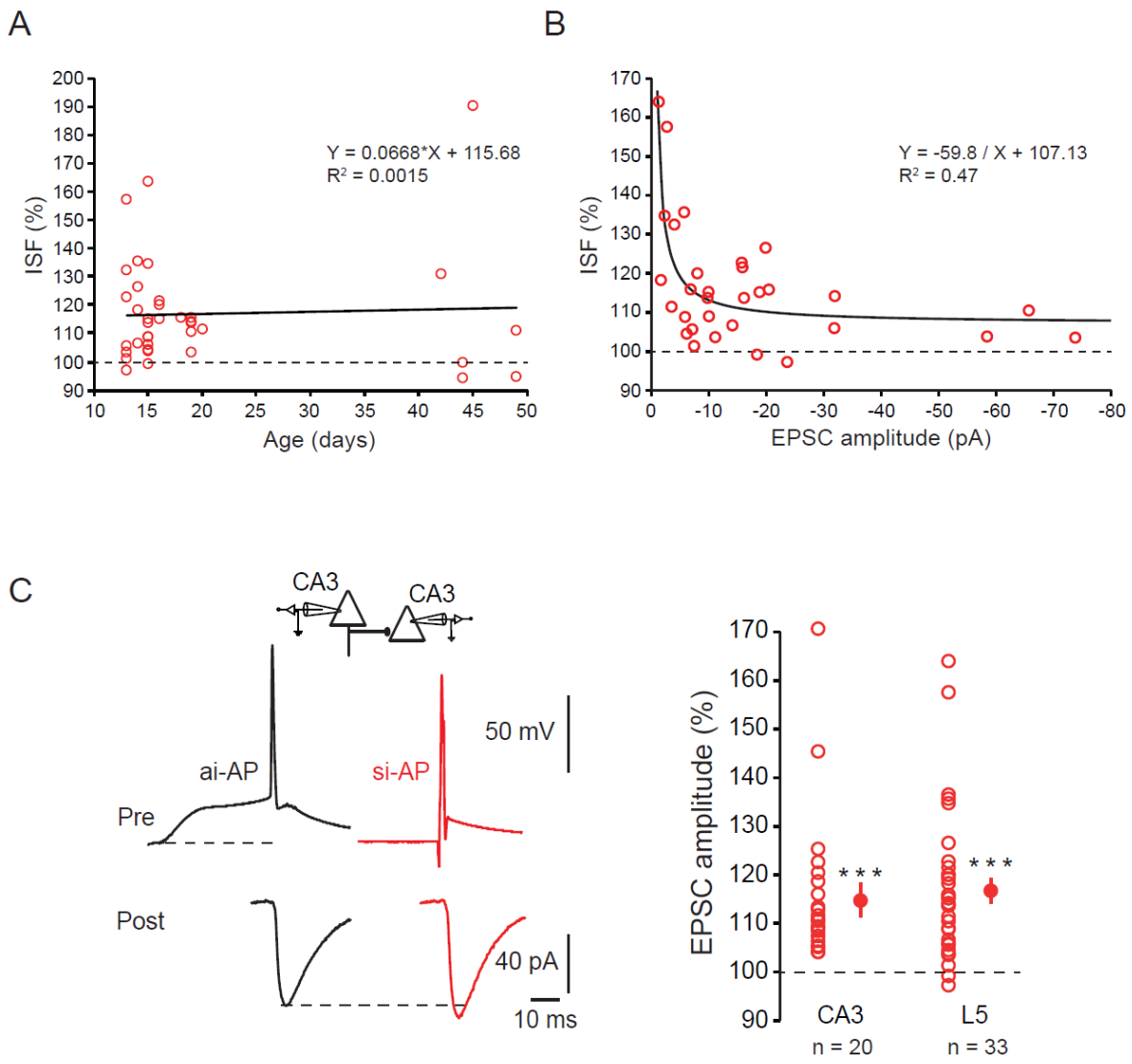

Fig. S2. Characteristics of ISF.

A. Plot of ISF as a function of age. Black line, linear regression (y = -1.04*x + 132.42, R^2 = 0.022). **B**. Plot of ISF as a function of EPSC amplitude. Black curve, regression (y = -70.37/x + 107.67, R^2 = 0.322). **C**. ISF at CA3-CA3 synapses. Left, representative example of electrophysiological recordings from a connected pair of CA3 neurons. Note the increase in postsynaptic response amplitude evoked by an action potential produced by synchronous-like input (red). Right, comparison of ISF in CA3 (n = 20) and L5 (n = 33) neurons (plots of EPSC amplitude evoked by synchronous-like inputs have been normalized to those evoked by asynchronous-like inputs). Resting membrane potential of the presynaptic neuron: -75 mV. ***: Wilcoxon test, p<0.001.

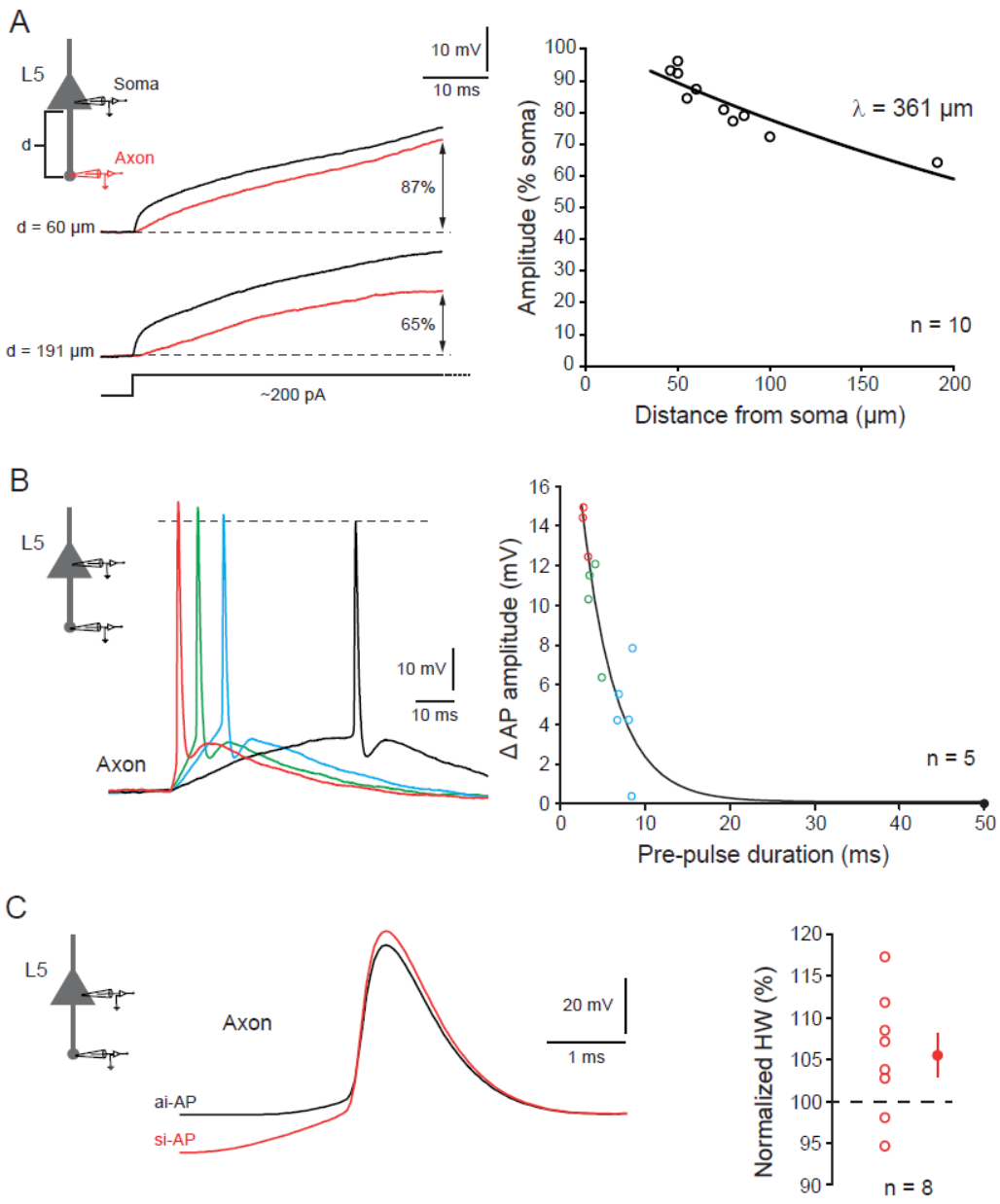

Fig. S3. Soma-axon recording: spatial and temporal properties.
A. Attenuation of subthreshold depolarization along the axon. Left, voltage traces recorded simultaneously in the soma (black) and the axon (red) upon current injection in the cell body. Note the larger attenuation observed for the longest axonal recording distance. Resting membrane potential: -80 mV. Right panel, exponential fit of the depolarization measured in the axon normalized to that measured in the soma ($y = 102.6 * e^{-x/\lambda}$, with λ = 361 µm, R^2 = 0.83). **B.** Time-course of enhanced spike amplitude recorded in the axon. Left, action potential evoked by asynchronous-like (black), intermediate-like (blue & green), and synchronous-like (red) inputs. Resting membrane potential: -80 mV. Right, variation in spike amplitude as a function of spike latency (5 axons). Each data point of the same color represents averaged values in a single recording. Note the rapid modulation in spike amplitude (black line, exponential regression ($y = -0.098 + 28.12 * e^{-x/\tau}$, with τ = 4.0 ms, R^2 = 0.91). **C.** No change in axonal spike duration was observed during ISF (p>0.1). Left, representative example (black trace: ai-AP, red trace: si-AP). Right, pooled data.

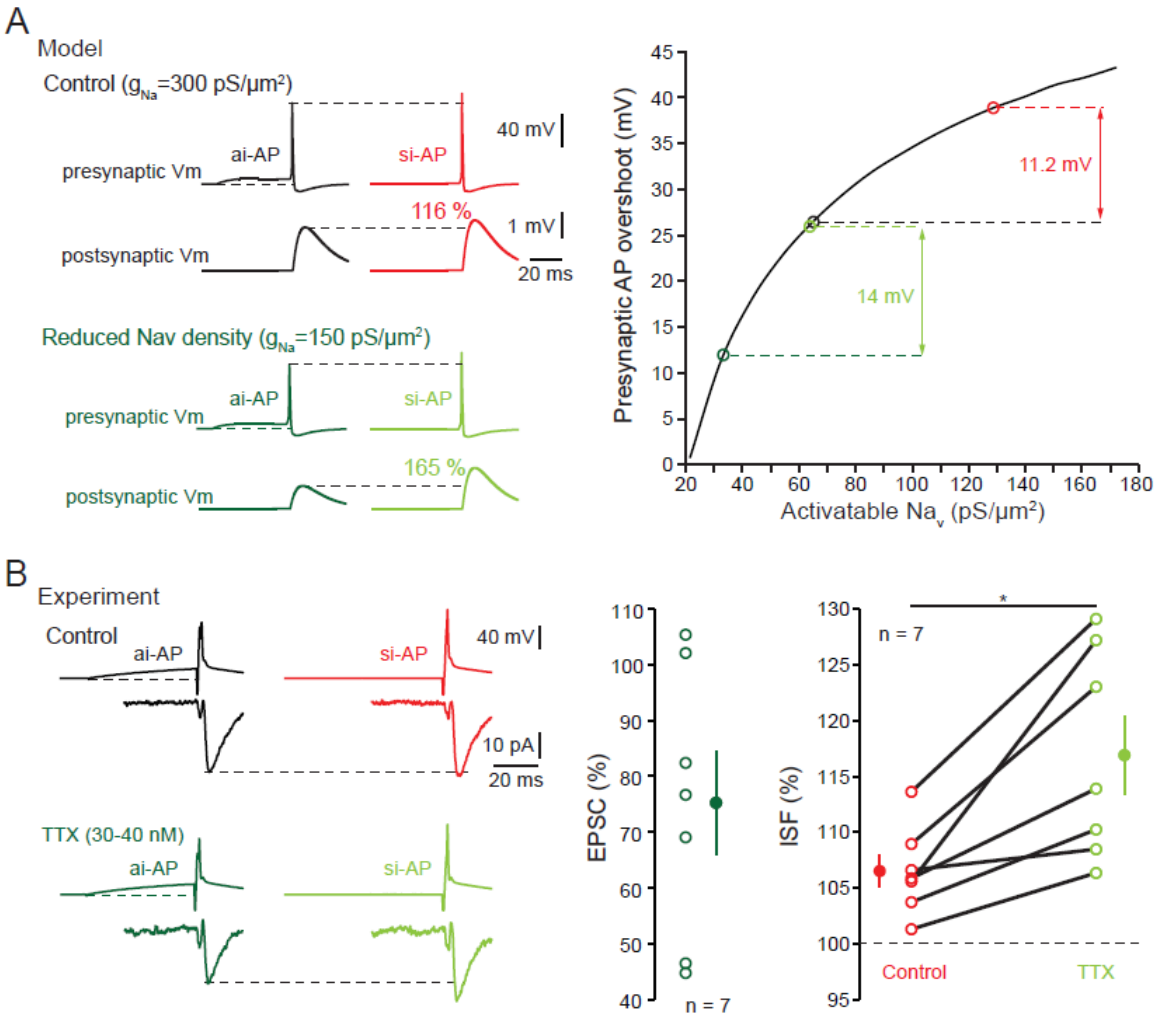

Fig. S4. Modulation of ISF by Na_v density.

A. Modeled reduction of Na_v density and enhancement of ISF. Top left, control conditions (g_{Nav} = 300 pS/µm^2). Bottom left, the reduction of Na_v density by 50% (g_{Nav} = 150 pS/µm^2) enhances the modulation of presynaptic spike amplitude and ISF. Resting membrane potential of the presynaptic bouton: -78 mV. Right, presynaptic spike amplitude as a function of activatable Na_v channel density. Note that the non-linear relationship accounts for increased modulation of spike amplitude during ISF (red in control condition and light green in low Na_v channel density condition). **B.** Experimental verification of theoretical prediction. Top left, ISF in control condition. Bottom left, enhancement of ISF in the presence of tetrodotoxin (TTX). Resting membrane potential of the presynaptic cell: -77 mV. Middle, plot of EPSC amplitude reduction caused by TTX. Right, pooled data showing the increase of ISF in TTX.

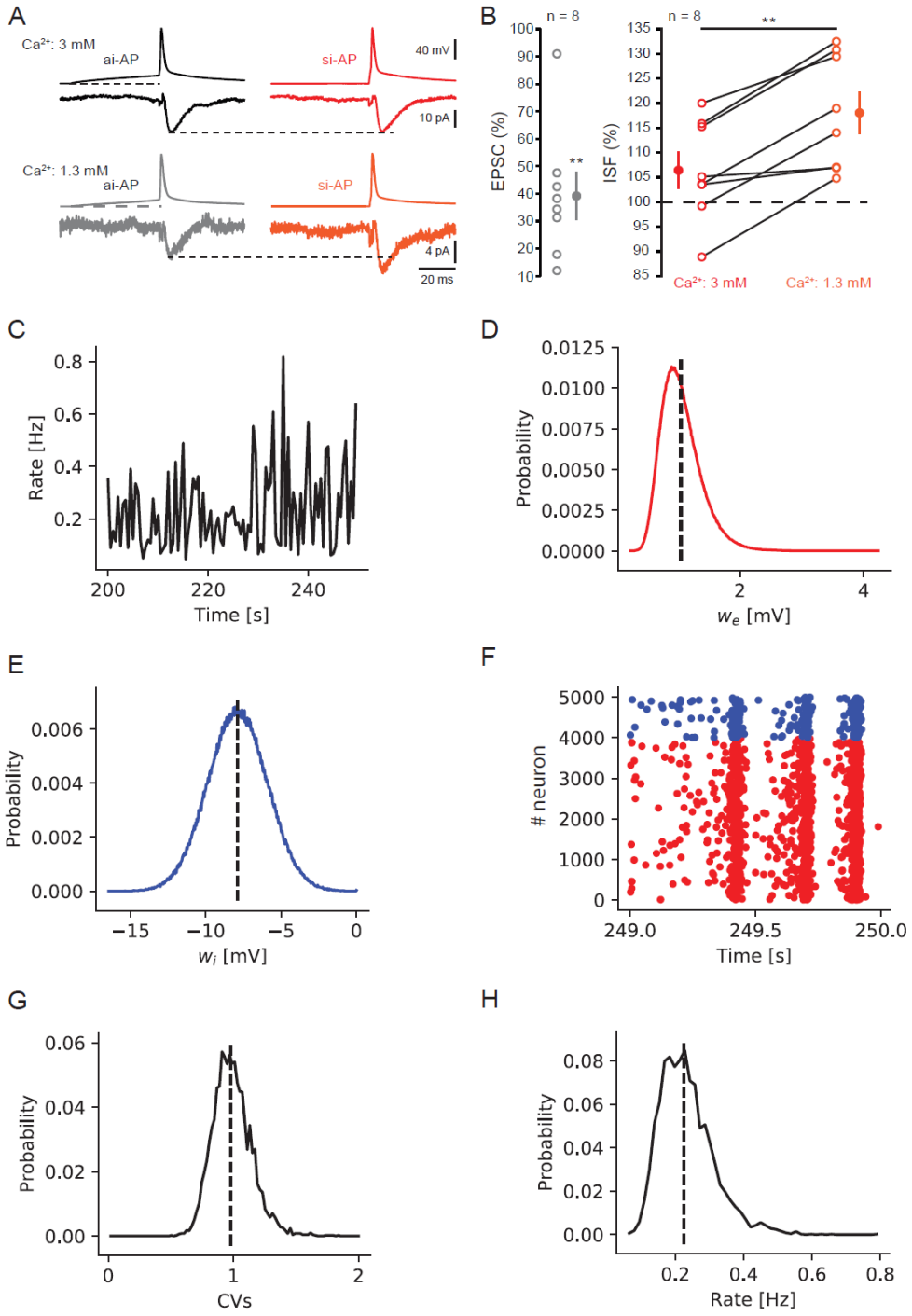

Fig. S5. ISF in physiological external concentration of Ca^{2+} and dynamics of the balanced network.
A. Top, lack of ISF in 3 mM Ca^{2+}. Bottom, ISF in 1.3 mM Ca^{2+} (same connection). Resting membrane potential: -81 mV. **B.** Left, plot of EPSC amplitude in 1.3 mM Ca^{2+} normalized to the control situation (3 mM Ca^{2+}). Right, pooled data of ISF in 3 mM Ca^{2+} and 1.3 mM Ca^{2+}. **C.** Firing rate of the whole network during 50 s. **D.** Distribution of the excitatory weights. Dash dotted line shows the mean weight $< w_{exc} > = 1\,mV$. **E.** Distribution of the inhibitory synaptic weights. Dash-dotted line shows the mean weight. **F.** Raster plot of the activity during 1 second for all neurons (excitatory in red, inhibitory in blue). **G.** Distribution of the coefficients of variation for the inter-spike intervals, over all neurons in the network. Dash-dotted line shows the mean CV, equal to 1. **H.** Distribution of the firing rates over all neurons in the network. Dash dotted line shows the mean at 0.21Hz.

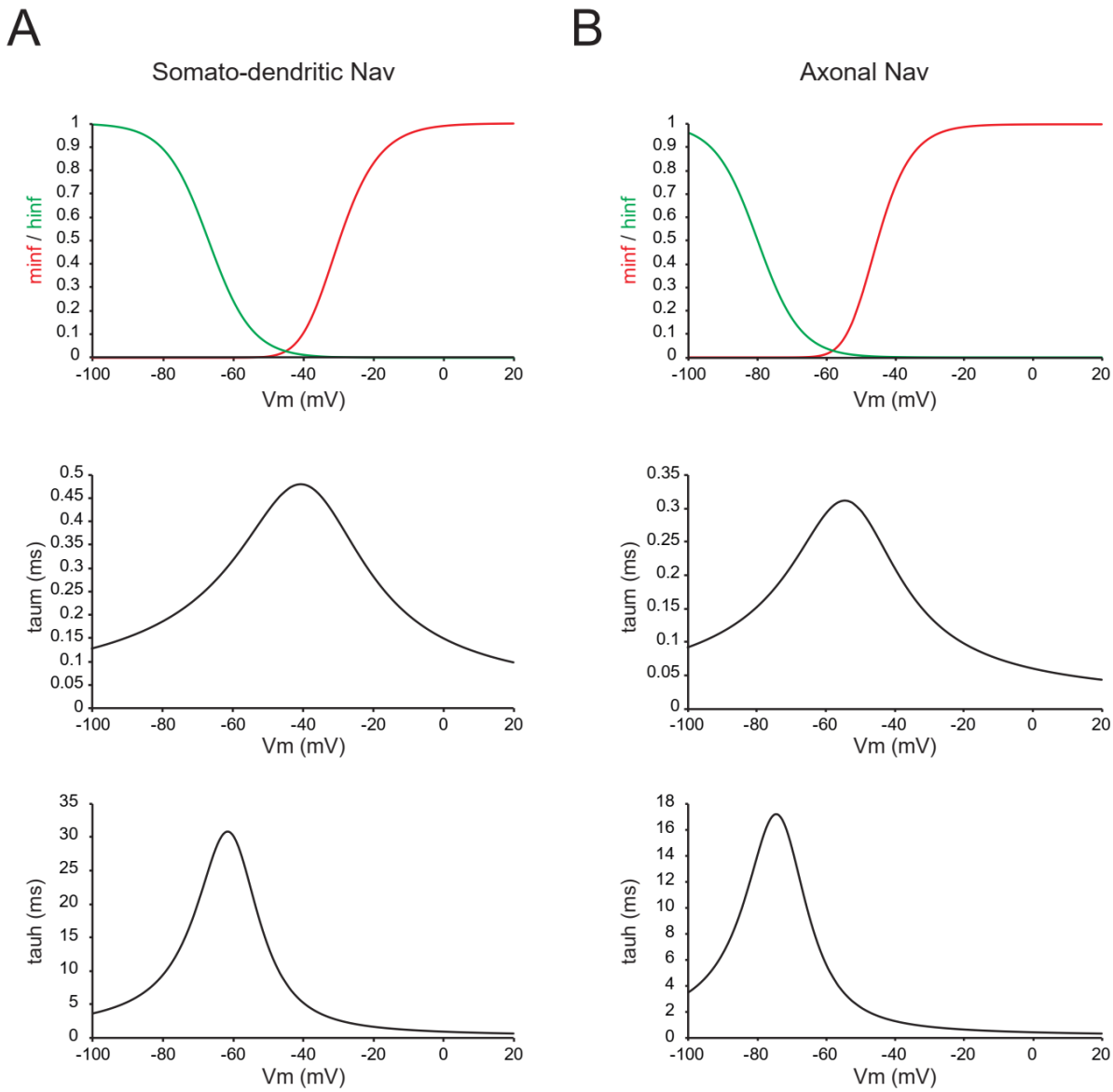

Fig. S6. Biophysics of sodium channels in the compartmental model
A. Biophysics of somato-dendritic channels. B. Biophysics of axonal channels. These biophysics were taken from Hu et al., 2009.

	Dendrite	Soma	Hillock	AIS	Axon	Terminal
Passive conductance (S/cm^2)	$3.33*10^{-5}$	$3.33*10^{-5}$	$3.33*10^{-5}$	$3.33*10^{-5}$	$3.33*10^{-5}$	$3.33*10^{-5}$
$g_{Na1.2}$ (S/cm^2)	0.008	0.008	0.256	0.3072-0	0	0
$g_{Na1.6}$ (S/cm^2)	0	0	0	0-0.1865	0.03	0.03
g_{Kv1} (S/cm^2)	0	0	0	0	0.003	0.003
g_{KDR} (S/cm^2)	0.01	0.01	0.01	0.01	0.01	0.01
g_{Ca} (S/cm^2)	0	0	0	0	0	0.0054

Table S1. Model parameters